Lorentz canoncial forms of two-qubit states

Sudha

Department of Physics, Kuvempu University, Shankaraghatta-577 451, Karnataka, India Inspire Institute Inc., Alexandria, Virginia, 22303, USA *

A. R. Usha Devi

Department of Physics, Bangalore University, Bangalore-560 056, India Inspire Institute Inc., Alexandria, Virginia, 22303, USA.*

B. N. Karthik

Department of Physics, Bangalore University, Bangalore-560 056, India

H. S. Karthik and Akshata Shenoy H

International Centre for Theory of Quantum Technologies, University of Gdánsk, Gdánsk, Poland[†]

K. S. Mallesh

Regional Institute of Education (NCERT), Mysuru 570006, India ‡

A. V. Gopala Rao

Department of Studies in Physics, University of Mysore, Manasagangotri, Mysore-570 006, India[§]

(Dated: February 15, 2024)

The Bloch sphere provides an elegant way of visualizing a qubit. Analogous representation of the simplest composite state of two-qubits has attracted significant attention. Here we present a detailed mathematical analysis of the real-matrix parametrization and associated geometric picturization of arbitrary two-qubit states - up to their local SL(2C) equivalence – in terms of canonical ellipsoids inscribed within the Bloch sphere.

CONTENTS Lorentz transformations 2 A. Lorentz transformation on the real parametrization matrix Λ of two-qubit density matrices 3 I. Introduction 2 B. Real symmetric matrix $\Omega = \Lambda^T G \Lambda$ 3 II. Real parametrization of two-qubit density matrix and III. Spectral analysis of the matrix $\mathbf{G}\,\Omega$ 4 A. G-eigenvalues of Ω 4 B. G-eigenvectors of Ω 5 * tthdrs@gmail.com † karthik.hs@ug.edu.pl IV. Geometrical visualization of two-qubit states 7 [‡] ksmallesh@gmail.com § garakali@gmail.com 7 V. Illustrative examples

VI. Summary

VII. Acknowledgments 11

References 11

I. INTRODUCTION

Bloch sphere (Bloch, 1946), named after the physicist Felix Bloch, provides a geometrical embedding for qubit (quantum two-level system). Pure states of a qubit constitutes the entire Bloch sphere and mixed states lie inside. This picture has been utilized widely in quantum dynamics in general and quantum information processing in particular. Extension of similar picturization for higher-dimensional state spaces have been proposed (Bengtsson and Zyczkowski, 2006; Goyal et al., 2016; Kimura and Kossakwski, 2005a; Rau, 2021). These studies point towards the emergence of intricate geometric structures as the Hilbert space dimension goes up and this hinders their utility in the field of quantum information processing. Given the key role played by entanglement in quantum information processing, there have been dedicated efforts to unravel geometric features associated with the simplest bipartite system viz., two-qubit state (Avron et al., 2007; Gamel, 2016; Horodecki and Horodecki, 1996; Jevtic et al., 2014; Milne et al., 2014; Rau, 2021; Sudha et al., 2020; Verstraete et al., 2001; Verstraete, 2002). Visualization of two-qubit states as ellipsoids inscribed inside the Bloch ball is found to be useful to understand quantum correlation features (Jevtic et al., 2014; Milne et al., 2014; Sudha et al., 2020; Verstraete, 2002). Investigation of the geometry of twoqubit states depends crucially on the local invertible linear transformations. In particular, restricting to local invertible qubit transformations represented by 2×2 complex matrices with determinant 1, enables one to exploit the homomorphism between the groups SL(2,C) and Lorentz group SO(3.1). In this paper we address the intricate and subtle features of Lorentz canonical forms associated with two-qubit states, which lead to their geometrical visualization as ellipsoids inside the Bloch ball.

We organize our paper in the following manner: Section II is devoted to the discussion of 4×4 real matrix parametrization Λ of two-qubit density matrix ρ_{AB} and its transformation properties when individual qubits are subjected to $\mathrm{SL}(2,\mathbb{C})$ operations. Introduction of a real symmetric 4×4 matrix $\Omega=\Lambda^T G\Lambda$, where $G=\mathrm{diag}\,(1,-1,-1,-1)$ and the spectral analysis of the matrix $G\Omega$ constitutes the content of Section III. Based on the analysis of the eigenvalues and eigenvectors of $G\Omega$ we arrive at two types of the Lorentz canonical forms of Λ and the associated canonical forms of the two-qubit density matrices on the sharing the same $\mathrm{SL}(2,\mathbb{C})$ orbit in Section IV, which also contains details on the geometrical embedding of the two-qubit states as canonical

steering ellipsoids inside the Bloch sphere. Section V has illustrative physical examples capturing the spectral analysis of $G\Omega$ and the geometrical visualization of the two-qubit density matrix ρ_{AB} . We summarize our results in Section VI.

II. REAL PARAMETRIZATION OF TWO-QUBIT DENSITY MATRIX AND LORENTZ TRANSFORMATIONS

Let us denote the Pauli basis

$$\sigma_{\mu} \equiv \{ \sigma_0 = \mathbb{1}_2, \sigma_0 = \sigma_x, \sigma_2 = \sigma_y, \sigma_3 = \sigma_z \}$$
 (1)

where $\mathbb{1}_2$, denotes 2×2 identity matrix and $\sigma_x, \sigma_y, \sigma_z$ are the Pauli spin matrices. Any arbitrary two-qubit state ρ_{AB} can be expressed in the Pauli basis $\{\sigma_{\mu} \otimes \sigma_{\nu}, \mu, \nu = 0, 1, 2, 3\}$ as,

$$\rho_{AB} = \frac{1}{4} \sum_{\mu,\nu=0}^{3} \Lambda_{\mu\nu} \left(\sigma_{\mu} \otimes \sigma_{\nu} \right) \tag{2}$$

where

10

$$\Lambda_{\mu\nu} = \text{Tr} \left[\rho_{AB} \left(\sigma_{\mu} \otimes \sigma_{\nu} \right) \right]. \tag{3}$$

Hermiticity of the density matrix implies that $\Lambda_{\mu\nu}$ are real for all μ, ν .

Expressed in the 2×2 block form, the 4×4 real matrix Λ (see (3)) assumes the following compact form,

$$\Lambda = \begin{pmatrix} 1 & \mathbf{b}^T \\ \mathbf{a} & T \end{pmatrix}. \tag{4}$$

Here the superscript "T" denotes matrix transposition; $\mathbf{a} = (a_1, a_2, a_3)^T$, $\mathbf{b} = (b_1, b_2, b_3)^T$ denote Bloch vectors of the reduced density matrices of qubits A, B:

$$\rho_A = \text{Tr}_B(\rho_{AB})$$

$$= \frac{1}{2} \sum_{\mu=0}^3 a_{\mu} \, \sigma_{\mu}, \quad a_{\mu} = (1, \mathbf{a})$$
 (5)

$$\rho_B = \text{Tr}_A(\rho_{AB})$$

$$= \frac{1}{2} \sum_{\mu=0}^{3} b_{\mu} \sigma_{\mu}, \quad b_{\mu} = (1, \mathbf{b})$$
(6)

(7)

and T denotes the 3×3 real correlation matrix (Horodecki and Horodecki, 1996), elements of which are given by $t_{ij} = \text{Tr}(\rho_{AB} \, \sigma_i \otimes \sigma_j), \, i, j = 1, 2, 3$. The 4×4 real matrix Λ is thus characterized by 15 real parameters (3 each of the Bloch vectors \mathbf{a} , \mathbf{b} and 9 elements of the correlation matrix T) and it provides a faithful real matrix parametrization of the two-qubit density matrix ρ_{AB} .

A. Lorentz transformation on the real parametrization matrix $\boldsymbol{\Lambda}$ of two-qubit density matrices

Under the action of local invertible operations $A, B \in SL(2, \mathbb{C})$ on individual qubits the two-qubit density operator transforms as (Jevtic *et al.*, 2014; Sudha *et al.*, 2020; Verstraete *et al.*, 2001)

$$\rho_{AB} \longrightarrow \widetilde{\rho}_{AB} = \frac{(A \otimes B) \ \rho_{AB} \ (A^{\dagger} \otimes B^{\dagger})}{\operatorname{Tr} \left[\rho_{AB} \ (A^{\dagger} A \otimes B^{\dagger} B)\right]}, \quad (8)$$

In view of the homomorphism between the groups $SL(2, \mathbb{C})$ – elements of which are 2×2 complex invertible matrices with determinant 1 – and the orthochronous proper Lorentz group SO(3,1) – consisting of 4×4 real matrices L which preserve the Mikowski metric $G=\mathrm{diag}\,(1,-1,-1,-1,-1)$ such that $L^T\,G\,L=G$ and $\det\,L=1$ – there exists a correspondence (Srinivasa Rao , 2011) $\pm A\mapsto L_A,\,\pm B\mapsto L_B,\,$ for $A,\,B\in\mathrm{SL}(2,\mathbb{C})$ and $L_A,\,L_B\in\mathrm{SO}(3,1)$. More specifically, the Pauli basis matrices $\sigma_\mu\otimes\sigma_\nu,\mu,\nu=0,1,2,3$ transform under $\mathrm{SL}(2,\mathbb{C})\otimes\mathrm{SL}(2,\mathbb{C})$ as

$$(A \otimes B)(\sigma_{\mu} \otimes \sigma_{\nu})(A^{\dagger} \otimes B^{\dagger}) = A \, \sigma_{\mu} A^{\dagger} \otimes B \, \sigma_{\nu} B^{\dagger}$$
$$= \sum_{\alpha,\beta=0,1,2,3} (L_{A})_{\alpha\mu} \, (L_{B})_{\beta\nu} \, \sigma_{\alpha} \otimes \sigma_{\beta}. \tag{9}$$

Thus, the transformation $\rho_{AB} \to \tilde{\rho}_{AB}$ on the two-qubit state is equivalent to the Lorentz transformation (up to normalization) of the real matrix Λ :

$$\Lambda \longrightarrow \tilde{\Lambda} = L_A \Lambda L_B^T. \tag{10}$$

Obviously $\tilde{\Lambda}$, obtained after the Lorentz transformations L_A, L_B on Λ (see (10)), parametrizes the two-qubit density matrix $\tilde{\rho}_{AB} = \frac{(A \otimes B) \, \rho_{AB} \, (A^{\dagger} \otimes B^{\dagger})}{\text{Tr}[\rho_{AB} \, (A^{\dagger} A \otimes B^{\dagger} B)]}$.

B. Real symmetric matrix $\Omega = \Lambda^T G \Lambda$

Let us denote the set of all non-negative operators acting on the qubit Hilbert space \mathbb{C}_2 by $\mathcal{P}^+ := \{P|P \geq 0\}$. Any element $P \in \mathcal{P}^+$ can be expressed in the Pauli basis $\sigma_{\mu} = (\mathbb{1}_2, \sigma_1, \sigma_2, \sigma_3)$ as

$$P = \frac{1}{2} \sum_{\mu} p_{\mu} \sigma_{\mu} \tag{11}$$

where

$$p_{\mu} = \text{Tr}(P \, \sigma_{\mu}), \mu = 0, 1, 2, 3$$

are the four real parameters characterizing P. With every $P \in \mathcal{P}^+$, one can associate a Minkowski fourvector (Srinivasa Rao , 2011; Synge , 1972)

$$\mathbf{p} = (p_0, p_1, p_2, p_3)^T.$$

Non-negativity $P \ge 0$ is synonymous to the conditions $\operatorname{Tr}(P) = p_0 > 0$ and $\det P = p_0^2 - p_1^2 - p_2^2 - p_3^2 \ge 0$ on the four-vector \mathbf{p} and thus P can be recognized as an element of a positive-operator valued measure (POVM).

In the language of Minkowski space, equipped with the metric

$$G = diag(1, -1, -1, -1)$$

the positivity $P \geq 0$ is synonymous to the four-vector norm condition $\mathbf{p}^T G \mathbf{p} \geq 0$, along with the restriction $p_0 > 0$ on zeroth component of the four-vector \mathbf{p} . In other words, the four-vector $\mathbf{p} = (p_0, p_1, p_2, p_3)^T$ of the POVM element P is either time-like $(\mathbf{p}^T G \mathbf{p} > 0)$ or null $(\mathbf{p}^T G \mathbf{p} = 0)$.

Let us consider the map

$$P \mapsto Q = 2 \operatorname{Tr}_B \left[\rho_{AB} \left(\mathbb{1}_2 \otimes P \right) \right] \tag{12}$$

from the set of all non-negative operators $\mathcal{P}^+:=\{P\mid P\geq 0\}$ on the Hilbert space \mathcal{H}_B to the set of non-negative operators $\mathcal{Q}^+:=\{Q=2\operatorname{Tr}_B[\rho_{AB}\left(\mathbbm{1}_2\otimes P\right)]\}$. This map has the following physical interpretation: When Bob carries out a measurement on his qubit and obtains outcome linked with the POVM element P, Alice's qubit gets steered to the quantum state proportional to $Q=\operatorname{Tr}_B\left[\rho_{AB}\left(\mathbbm{1}_2\otimes P\right)\right]$.

It is readily seen that

$$Q = 2 \operatorname{Tr}_{B} \left[\rho_{AB} \left(\mathbb{1}_{2} \otimes P \right) \right]$$
$$= \frac{1}{2} \sum_{\nu} \left(\Lambda \mathbf{p} \right)_{\nu} \sigma_{\nu}$$
(13)

resulting in the Minkowski four-vector transformation

$$\mathbf{q} = \Lambda \,\mathbf{p}.\tag{14}$$

In other words, the map $P \mapsto Q$ is identical to the four-vector map $\Lambda : \mathbf{p} \mapsto \mathbf{q} = \Lambda \mathbf{p}$.

Clearly, the squared Minkowski norm of the four-vector \mathbf{q} is non-negative (i.e., the four-vector \mathbf{q} is either time-like or null). Thus,

$$\mathbf{q}^{T} G \mathbf{q} \ge 0 \implies \mathbf{p}^{T} \Lambda^{T} G \Lambda \mathbf{p} \ge 0$$
$$\implies \mathbf{p}^{T} \Omega \mathbf{p} \ge 0 \tag{15}$$

where

$$\Omega = \Lambda^T G \Lambda \tag{16}$$

denotes a real symmetric 4×4 matrix, associated with the real parametrization Λ of the two-qubit density matrix ρ_{AB} . Furthermore, positivity of the zeroth component of the four-vector \mathbf{p} (i.e., Tr(P) > 0) imposes that

$$p_0 > 0 \Longrightarrow q_0 = (\Lambda \mathbf{p})_0 > 0.$$
 (17)

The 4×4 real symmetric matrix $\Omega = \Lambda^T G \Lambda$ constructed from the real counterpart Λ of the two-qubit

density matrix ρ_{AB} plays a key role in our analysis and is inspired by the methods developed in classical polarization optics (Gopala Rao *et al.*, 1998a,b). Spectral analysis of the 4×4 matrix $G\Omega = G\Lambda^T G\Lambda$ results in the geometrical visualization of two-qubit states on the SL(2,C) orbit as ellipsoids inside the Bloch Ball.

III. SPECTRAL ANALYSIS OF THE MATRIX $\mathbf{G}\,\Omega$

We focus on the condition (see equations (15), (16) and (17))

$$\{\mathbf{q} = \Lambda \, \mathbf{p} | \mathbf{q}^T \, G \mathbf{q} = \mathbf{p}^T \, \Omega \, \mathbf{p} \ge 0, \quad q_0 > 0 \}$$
 (18)

Since every time-like four-vector can always be expressed as a sum of null four-vectors (Srinivasa Rao , 2011), we choose to confine ourselves to the set of null four-vectors

$$\left\{ \mathbf{p} \equiv \mathbf{p}_n = (1, \mathbf{x})^T, \quad \mathbf{x}^T \mathbf{x} = 1; \quad \mathbf{p}_n^T G \mathbf{p}_n = 0 \right\}$$
 (19)

without any loss of generality.

The non-negativity constraint (18) can thus be expressed as

$$\left\{\mathbf{q} = \Lambda \,\mathbf{p}_n | \mathbf{p}_n^T \, G \mathbf{p}_n = 0 \Longrightarrow \mathbf{q}^T \, G \mathbf{q} = \mathbf{p}_n^T \, \Omega \mathbf{p}_n \ge 0\right\} \tag{20}$$

where $\Omega = \Lambda^T G \Lambda = \Omega^T$.

Under the transformation (see equation (10)) $\Lambda \to \tilde{\Lambda} = L_A \Lambda L_B^T$, $L_A, L_B \in SO(3,1)$, the matrix $\Omega = \Lambda^T G \Lambda$ gets subjected to a Lorentz congruent operation:

$$\widetilde{\Omega} = \widetilde{\Lambda}^T G \widetilde{\Lambda}$$

$$= (L_A \Lambda L_B^T)^T G (L_A \Lambda L_B^T)$$

$$= L_B \Lambda^T L_A^T G L_A \Lambda L_B^T$$

$$= L_B \Lambda^T G \Lambda L_B^T$$

$$= L_B \Omega L_B^T$$
(21)

where we have used the metric-preserving property $L_A^T G L_A = G$ of $L_A \in SO(3,1)$.

With the help of the relation

$$GL = \left(L^T\right)^{-1}G$$

satisfied by Lorentz transformation matrix, it is easy to identify that

$$G\Omega = G\Lambda^T G\Lambda \tag{22}$$

undergoes a similarity transformation as follows:

$$G\Omega \longrightarrow GL\Omega L^{T}$$

$$= (L^{T})^{-1} G\Omega L^{T}. \tag{23}$$

It is thus clear that the eigenvalues of the 4×4 real matrix $G\Omega$ remain invariant under Lorentz transformation. We refer to the eigenvalues and eigenvectors of $G\Omega$ as G-eigenvalues and G-eigenvectors of the matrix Ω respectively. Detailed discussion on the spectral properties of the matrix $G\Omega$ associated with two-qubit states is presented in the following subsection.

A. G-eigenvalues of Ω

Let us express the matrix Ω in the block form

$$\Omega = \begin{pmatrix} \Omega_{00} & \boldsymbol{\omega}^T \\ \boldsymbol{\omega} & S \end{pmatrix} \tag{24}$$

where $\boldsymbol{\omega}^T = (\Omega_{01}, \, \Omega_{02}, \, \Omega_{03})$ and $S = S^T$ is a real, symmetric 3×3 matrix. We consider a simpler form of the matrix Ω with the help of Lorentz congruent transformations $\widetilde{\Omega} = L^T \Omega L$ (see equation (21)). To this end, we choose $L = 1 \oplus R$, where $R \in SO(3)$ is a 3×3 rotation matrix diagonalizing the real symmetric matrix S (see equation (24) i.e., $R S R^T = S_{\alpha} = \text{diag}(\alpha_1, \alpha_2, \alpha_3)$. Consequently, $\boldsymbol{\omega} \to R \boldsymbol{\omega}$. We thus obtain

$$\Omega \to \Omega_0 = L^T \Omega L = (1 \oplus R) \Omega (1 \oplus R^T) = \begin{pmatrix} n_0 & \mathbf{n}^T \\ \mathbf{n} & S_\alpha \end{pmatrix}$$
(25)

where we have denoted $\Omega_{00} = n_0$ and $R \boldsymbol{\omega} = \mathbf{n} = (n_1, n_2, n_3)^T$.

We express the positivity condition $\mathbf{p}_n^T \Omega_0 \mathbf{p}_n \geq 0$ (see equation (20), where we consider the simpler structure Ω_0 given by equation (25):

$$D(\Omega_0; \mathbf{x}) = n_0 + 2 \mathbf{x}^T \mathbf{n} + \mathbf{x}^T S_\alpha \mathbf{x} \ge 0 \qquad (26)$$
$$\forall \mathbf{x}^T \mathbf{x} = 1.$$

For condition (26) to hold good, the absolute minima of the function $D(\Omega_0; \mathbf{x})$, or equivalently, *critical values* of $D(\Omega_0; \mathbf{x})$ should be non-negative. In order to find the critical values of $D(\Omega_0; \mathbf{x})$ we employ the Lagrange multiplier method and define

$$K(\Omega_0; \mathbf{x}) = D(\Omega_0; \mathbf{x}) + \lambda (\mathbf{x}^T \mathbf{x} - 1)$$
 (27)

where λ denotes the Lagrange multiplier.

Setting the partial derivatives of $K(\Omega_0; \mathbf{x})$ with respect to λ and x_i , i = 1, 2, 3 equal to zero at the critical values λ_c , \mathbf{x}_c i.e.,

$$\frac{\partial K(\Omega_0; \mathbf{x})}{\partial \lambda} \Big|_{\lambda_c, \mathbf{x}_c} = 0$$

$$\frac{\partial K(\Omega_0; \mathbf{x})}{\partial x_i} \Big|_{\lambda_c, \mathbf{x}_c} = 0, \quad i = 1, 2, 3$$
(28)

we obtain

$$(S_{\alpha} + \lambda_c \, \mathbb{1}_3) \, \mathbf{x}_c = -\mathbf{n}, \quad \mathbf{x}_c^T \, \mathbf{x}_c = 1 \tag{29}$$

or

$$x_{ci} = \frac{-n_i}{(\alpha_i + \lambda_c)}, \ i = 1, 2, 3.$$
 (30)

Substituting equation (30) and $\mathbf{x}_c^T \mathbf{x}_c = x_{c1}^2 + x_{c2}^2 + x_{c3}^2 = 1$ in equation (26) we arrive at the constrained critical values D_c of $D(\Omega_0; \mathbf{x})$:

$$D_c = n_0 - \lambda_c - \sum_{i=1}^{3} \left(\frac{n_i^2}{\lambda_c + \alpha_i} \right). \tag{31}$$

Let us consider

$$h(\lambda) = n_0 - \lambda - \sum_{i=1}^{3} \frac{n_i^2}{\lambda + \alpha_i}, \tag{32}$$

obtained by replacing λ_c in D_c (see equation (31)) by a continuous variable λ .

We list the following properties of the function $h(\lambda)$:

- 1. From equation (32) it is seen that $h(\lambda)$ has finite number of discontinuities positioned at $\lambda = -\alpha_i$, i = 1, 2, 3, whenever the corresponding $n_i \neq 0$.
- 2. From explicit evaluation we recognize that

$$h(\lambda) = -\frac{\det(G\Omega_0 - \lambda \mathbb{1}_4)}{\det(S_\alpha + \lambda \mathbb{1}_3)}.$$
 (33)

This leads to an important observation that the real roots of $h(\lambda)$ are nothing but the G-eigenvalues of the matrix Ω_0 :

$$\det(G\Omega_0 - \lambda \mathbb{1}_4) = -h(\lambda) \det(S_\alpha + \lambda \mathbb{1}_3)$$

$$= -h(\lambda) (\alpha_1 + \lambda)(\alpha_2 + \lambda)(\alpha_3 + \lambda).$$
(34)

- 3. The function $h(\lambda)$ changes sign across its discontinuity and is positive to the immediate left and negative to the immediate right of a discontinuity. This implies that odd number of zeros (at least one) exist between any two discontinuities of $h(\lambda)$.
- 4. From equation (32) it may be noticed that $h(\lambda) \to \infty$ as $\lambda \to -\infty$ and $h(\lambda) \to -\infty$ as $\lambda \to \infty$. Based on this observation, together with the behaviour of $h(\lambda)$ near a given discontinuity, it is inferred that even number of zeros (at least two) lie in the interval $(\alpha_{\text{max}}, \infty)$, where α_{max} is the largest of $(\alpha_1, \alpha_2, \alpha_3)$.
- 5. As $h(\lambda) \to -\infty$ as $\lambda \to \infty$ and the largest zero λ_{\max} occurs in the interval (α_{max}, ∞) , the slope of $h(\lambda)$ at λ_{\max} is either negative or zero.

Depending on the number of non-zero values of n_1, n_2, n_3 and based on the degeneracies $\alpha_1, \alpha_2, \alpha_3$, there exist 20 possible situations, each with different number of discontinuities and zeros of the function $h(\lambda)$: (i) none of n_1, n_2, n_3 are zero; (ii) one of n_1, n_2, n_3 is zero (i.e., $n_1 = 0, n_2, n_3 \neq 0$; $n_2 = 0, n_1, n_3 \neq 0$; $n_3 = 0, n_1, n_2 \neq 0$), (iii) two of n_1, n_2, n_3 are zero (i.e., $n_1, n_2 = 0 \neq n_3$; $n_2, n_3 = 0 \neq n_1$; $n_1, n_3 = 0 \neq n_2$), (iv) $n_1 = n_2 = n_3 = 0$.

Each of these 4 cases fall under 5 different subclasses corresponding to the degeneracies of $\alpha_1, \alpha_2, \alpha_3$: non-degenerate i.e., (A) $\alpha_1 \neq \alpha_2 \neq \alpha_3$, two-fold degenerate i.e., (B1) $\alpha_1 = \alpha_2 \equiv \alpha \neq \alpha_3$, (B2) $\alpha_1 \neq \alpha_2 = \alpha_3 \equiv \alpha$, (B3) $\alpha_1 = \alpha_3 \equiv \alpha \neq \alpha_2$, and fully degenerate i.e., (C) $\alpha_1 = \alpha_2 = \alpha_3 = \alpha$.

Associated with these $4 \times 5 = 20$ distinct possibilities one may list the number of discontinuities and zeros of the function $h(\lambda)$. More specifically, it is seen that if $k \leq 3$ denote the finite number of distinct discontinuities of the function $h(\lambda)$, the function $h(\lambda)$ must have, at least k+1 real zeros. When there are two distinct discontinuities (k=2) at least one real zero of $h(\lambda)$ occurs between them and two zeros (either distinct or doubly repeated) appear in the region $(\alpha_{\text{max}}, \infty)$. Thus, 1+2=3 real zeros exist for $h(\lambda)$ when k=2.

In order to investigate the number k of discontinuities and its association with the number of zeros of $h(\lambda)$, we express the characteristic polynomial $\phi(\lambda) = \det(G\Omega_0 - \lambda \mathbb{1}_4)$ of $G\Omega_0$ as

$$\phi(\lambda) = \phi_1(\lambda) g(\lambda) h(\lambda) \tag{35}$$

in terms of two simple poynomials $\phi_1(\lambda)$ and $q(\lambda)$ such that (i) they have real roots; (ii) they are finite at every zero of the function $h(\lambda)$. Explicit structure of the polynomials $\phi_1(\lambda)$, $q(\lambda)$ and $h(\lambda)$ in each of the 20 different cases is given in Table 1. Based on careful examination of the characteristic equation $\phi(\lambda) = \det(G\Omega_0 - \lambda \mathbb{1}_4) = 0$ of $G\Omega_0$ and the explicit structures of $\phi_1(\lambda)$, $g(\lambda)$, $h(\lambda)$ in each of the 20 cases listed in Table 1, we reach the following conclusion: If r denotes the number of roots of $\phi_1(\lambda)$ and k denotes the number of discontinuities of $h(\lambda)$, then r+k+1=4 in all 20 cases. It is found that whenever the number of zeros k+1 of $h(\lambda)$ is less than 3 (or in turn, the number k of discontinuities exhibited by the function $h(\lambda)$ is less than 2), then the roots of the polynomial $\phi_1(\lambda)$ determine the remaining r number of G-eigenvalues of Ω_0 . This in turn culminates in the determination of all four G-eigenvalues λ_{μ} , $\mu = 0, 1, 2, 3$ of the 4×4 matrix Ω_0 .

B. G-eigenvectors of Ω

Having identified that the G-eigenvalues of Ω_0 are real roots of the function $h(\lambda)$, we proceed to investigate the explicit behaviour of zeros of $h(\lambda)$ so that the Lorentz nature of the G-eigenvectors of Ω_0 can be discerned. To this end we highlight the following features of the G-eigenvectors of Ω_0 – ascertained from the behaviour of the function $h(\lambda)$:

1. Let us denote the *G*-eigenvector associated with the *G*-eigenvalue λ of the matrix Ω by $X = (a, b, c, d)^T$. By solving the eigenvalue equation

$$G\Omega_0 X = \lambda X$$
 i.e.,

$$(n_0 - \lambda_0) a + n_1 b + n_2 c + n_3 d = 0,$$

$$n_1 a + (\alpha_1 + \lambda) b = 0,$$

$$n_2 a + (\alpha_2 + \lambda) c = 0,$$

$$n_3 a + (\alpha_3 + \lambda) d = 0.$$
 (36)

we obtain the explicit form of the G-eigenvector X:

$$X = \left(1, -\frac{n_1}{(\lambda + \alpha_1)}, -\frac{n_2}{(\lambda + \alpha_2)}, -\frac{n_3}{(\lambda + \alpha_3)}\right)^T.$$
(37)

2. Derivative of the function $h(\lambda)$ (see equation (32)) with respect to λ at one of its zeros is given by

$$h'(\lambda) = -1 + \sum_{i} \frac{n_i^2}{(\lambda + \alpha_i)^2}.$$
 (38)

We identify a striking connection

$$X^T G X = -h'(\lambda). \tag{39}$$

between the Minkowski norm of the G-eigenvector X (see equation (37)) associated with the G-eigenvalue λ of Ω_0 and the derivative $h'(\lambda)$. Thus, Minkowski space nature of the G-eigenvector (timelike, null, space-like) of Ω_0 essentially depends on the sign of the derivative $h'(\lambda)$ of the function $h(\lambda)$ at its zeros.

3. Recall that $h(\lambda) \to \mp \infty$ as $\lambda \to \pm \infty$. Furthermore, $h(\lambda)$ has at least two zeros in the region (α_{\max}, ∞) (see property 4 of subsection IIIA). Let us denote the largest zero of $h(\lambda)$ (i.e., largest G-eigenvalue of Ω_0) by λ_0 . Since the largest zero λ_0 appears in the interval (α_{\max}, ∞) , the slope $h'(\lambda_0)$ of the function $h(\lambda)$ at λ_0 is either negative or zero. From equation (39) it is seen that the G-eigenvector X_0 belonging to the largest eigenvalue λ_0 of Ω_0 obeys $X_0^T G X_0 \geq 0$. In other words, the G-eigenvector X_0 associated with the highest G-eigenvalue λ_0 of Ω_0 is either a time-like four-vector (if $h'(\lambda_0) > 0$) or null four-vector (if $h'(\lambda_0) = 0$).

It also follows that the largest G-eigenvalue λ_0 of Ω_0 is two-fold degenerate when $h'(\lambda_0) = 0$, i.e., when X_0 is a null four-vector.

- 4. Note that at least one zero must exist between any two discontinuities of $h(\lambda)$. The tangent $h'(\lambda_r)$ should necessarily be positive for $\lambda_r < \lambda_0$ and hence it is clear from (39) that the G-eigenvectors X_r of Ω_0 are space-like four-vectors.
- 5. A tetrad (X_0, X_1, X_2, X_3) consisting of one timelike and three space-like G-eigenvectors of Ω_0 constitute the columns of a Lorentz matrix (Srinivasa

Rao, 2011) $L_{Ic} \in SO(3,1)$ which ensures the transformation $\Omega_0 \to \Omega_{Ic} = L_{Ic} \Omega_0 L_{Ic}^T = \text{diag} (\lambda_0 - \lambda_1, -\lambda_2, -\lambda_3), \quad \lambda_0 \geq \lambda_1 \geq \lambda_2 \geq \lambda_3 \geq 0$, when the G-eigenvector X_0 is time-like (i.e., $h'(\lambda_0) < 0$).

6. When the highest G-eigenvalue λ_0 of Ω_0 is doubly degenerate and the corresponding G-eigenvector is null $(X_0^T G X_0 = 0)$, one obtains a triad of G-eigenvectors, consisting of one null and two spacelike four-vectors. Using this triad it is possible (Gopala Rao et al., 1998a; Srinivasa Rao, 2011; Sudha et al., 2020) to construct a Lorentz matrix L_{IIc} such that a non-diagonal canonical form (Sudha et al., 2020) is realized under the transformation $\Omega_0 \to \Omega_{IIc} = L_{IIc} \Omega_0 L_{IIc}^T$:

$$\Omega_{IIc} = \begin{pmatrix}
\chi_0 & 0 & 0 & \chi_0 - \lambda_0 \\
0 & -\lambda_1 & 0 & 0 \\
0 & 0 & -\lambda_2 & 0 \\
\chi_0 - \lambda_1 & 0 & 0 & \chi_0 - 2\lambda_0
\end{pmatrix},$$

$$\chi_0 = \left(L_{IIc} \Omega_0 L_{IIc}^T\right)_{00} \tag{40}$$

where $\lambda_0 \geq \lambda_1 \geq \lambda_2 \geq 0$. It is then realized that positivity of the associated two-qubit density matrix ρ_{AB} demands (Sudha *et al.*, 2020) that the *G*-eigenvalues $\lambda_1 = \lambda_2$. Therefore the *G*-eigenvalues λ_0 and λ_1 are two-fold degenerate in this case.

In summary, the matrix $\Omega = \Lambda^T G \Lambda$ associated with a two-qubit density matrix ρ_{AB} possesses either

(i) a time-like G-eigenvector belonging to its largest G-eigenvalue λ_0 and three space-like G-eigenvectors

OR

- (ii) a null G-eigenvector belonging to doubly degenerate eigenvalue λ_0 and two space-like G-eigenvectors associated with the remaining G-eigenvalue $\lambda_1 = \lambda_2$.
- (iii) A tetrad (X_0, X_1, X_2, X_3) consisting of one timelike and three space-like G-eigenvectors of Ω_0 form the columns of a Lorentz matrix L_{Ic} , which enables a transformation $\Omega_0 \to \Omega_{Ic} = L_{Ic} \Omega L_{Ic}^T =$ diag $(\lambda_0, -\lambda_1, -\lambda_2, -\lambda_3)$ of Ω_0 to a diagonal canonical form.
- (iv) The traid (X_0, X_1, X_2) consisting of one null and two space-like G-eigenvectors allows for the construction of a Lorentz matrix (Sudha *et al.*, 2020) L_{IIc} , which transform Ω_0 to its non-diagonal canonical form Ω_{IIc} given by equation (40), with $\lambda_1 = \lambda_1$.
- (v) The G-eigenvalues of Ω_0 are non-negative.

IV. GEOMETRICAL VISUALIZATION OF TWO-QUBIT STATES

Associated with the diagonal canonical form Ω_{Ic} one obtains the Lorentz canonical form Λ_{Ic} for the real parametrization Λ of the two-qubit density matrix ρ_{AB} :

$$\Lambda \longrightarrow \Lambda_{Ic} = \operatorname{diag}\left(1, \sqrt{\frac{\lambda_1}{\lambda_0}}, \sqrt{\frac{\lambda_2}{\lambda_0}}, \pm \sqrt{\frac{\lambda_3}{\lambda_0}}\right)$$
 (41)

where the sign \pm is chosen depending on sign $(\det(\Lambda)) = \pm$.

Consequently, the two-qubit density matrix ρ_{AB} assumes the following SL(2,C) canonical form (Bell-diagonal):

$$\rho_{AB}^{Ic} = \frac{1}{4} \left(\sigma_0 \otimes \sigma_0 + \sum_{i=1,2} \sqrt{\frac{\lambda_i}{\lambda_0}} \, \sigma_i \otimes \sigma_i \, \pm \sqrt{\frac{\lambda_3}{\lambda_0}} \, \sigma_3 \otimes \sigma_3 \right).$$

The Lorentz canonical form Λ_{IIc} for the real parametrization Λ of two-qubit density matrix ρ_{AB} corresponding to the non-diagonal canonical form of Ω_0 (see equation (40)) is given by (Sudha *et al.*, 2020)

$$\Lambda \longrightarrow \Lambda_{IIc} = \begin{pmatrix} 1 & 0 & 0 & 1 - s_0 \\ 0 & s_1 & 0 & 0 \\ 0 & 0 & -s_1 & 0 \\ 0 & 0 & 0 & s_0 \end{pmatrix}$$
(43)

where $s_0 = \frac{\lambda_0}{\chi_0}$, $s_1 = \sqrt{\frac{\lambda_1}{\chi_0}}$ (see equation (40) for definition of χ_0).

Correspondingly, one obtains the $SL(2,\mathbb{C})$ canonical form for the two-qubit density matrix:

$$\rho_{AB}^{IIc} = \frac{1}{4} \left[\sigma_0 \otimes \sigma_0 + (1 - s_0) \sigma_0 \otimes \sigma_3 + s_1 (\sigma_1 \otimes \sigma_1 - \sigma_2 \otimes \sigma_2) + s_0 \sigma_3 \otimes \sigma_3 \right]$$

$$(44)$$

Let us consider projective valued measurements (PVM) on Bob's qubit by

$$P = \sum_{\mu=0}^{3} p_{\mu} \, \sigma_{\mu}, P > 0, \tag{45}$$

where

$$p_0 = 1, \mathbf{p} = (p_1, p_2, p_3), \quad \mathbf{p}^T \mathbf{p} = p_1^2 + p_2^2 + p_3^2 = 1.$$
 (46)

Local PVM on the Bob's qubit results in collapsed states of Alice's qubit:

$$\rho_{\mathbf{q}} = \frac{1}{p} \operatorname{Tr}_{B} \left[\rho_{AB} \left(\mathbb{1}_{2} \otimes P \right) \right]
= \frac{1}{2} \sum_{\mu} q_{\mu} \sigma_{\mu}, \ q_{\mu} = \frac{1}{p} \sum_{\mu} \Lambda_{\mu\nu} p_{\nu}$$
(47)

with probability

$$p = \text{Tr} \left[\rho_{AB} \, \left(\mathbb{1}_2 \otimes P \right) \right] = \sum_{\mu=0}^3 \, \Lambda_{0\,\mu} \, p_{\mu}.$$

For the Lorentz canonical form Λ_{Ic} (see (41)) of the two-qubit state ρ_{AB}^{Ic} steered Bloch points \mathbf{q} of Alice's qubit are given by

$$\mathbf{q} = \left(q_1 = \sqrt{\frac{\lambda_1}{\lambda_0}} \, p_1, \, q_2 = \sqrt{\frac{\lambda_2}{\lambda_0}} \, p_2, \, \sqrt{\frac{\lambda_3}{\lambda_0}} \, p_3\right)$$
 (48)

which obey the equation of an ellipsoid with semi-axes $(\sqrt{\lambda_1/\lambda_0}, \sqrt{\lambda_2/\lambda_0}, \sqrt{\lambda_3/\lambda_0})$ and center (0,0,0) inside the Bloch sphere:

$$\frac{\lambda_0 \, q_1^2}{\lambda_1} + \frac{\lambda_0 \, q_2^2}{\lambda_2} + \frac{\lambda_0 \, q_3^2}{\lambda_3} = 1. \tag{49}$$

(42) We refer to this as the canonical steering ellipsoid of the set of all two-qubit density matrices ρ_{AB} which lie on the SL(2,C) orbit of the Bell-diagonal state ρ_{AB}^{Ic} (see (42)).

Corresponding to the second Lorentz canonical form Λ_{IIc} (see (43)) one obtains canonical steering spheroid with its semi-axes lengths (s_1, s_1, s_0) and center $(0, 0, 1-s_0)$:

$$\frac{q_1^2 + q_2^2}{s_1^2} + \frac{q_3 - (1 - s_0)}{s_0^2} = 1. {(50)}$$

In other words a shifted spheroid, inscribed within the Bloch sphere, represents the set of two-qubit states ρ_{AB} , which are SL(2,C) equivalent to ρ_{AB}^{IIc} (see (44)).

V. ILLUSTRATIVE EXAMPLES

In this section we consider specific examples of twoqubit density matrices to illustrate the properties of $h(\lambda)$ (see Sec. III) and associated canonical steering ellipsoids. To this end, we begin with examples of real symmetric matrix Ω_0 given in equation (25) and construct the associated function $h(\lambda)$. Plot of $h(\lambda)$ as a function of the continuous variable λ depicts discontinuities and roots (G-eigenvalues) of the function. Lorentz canonical form of the 4×4 real parametrization matrix Λ and the corresponding $SL(2,\mathbb{C})$ canonical form of the two-qubit density matrix are given.

Example 1: Consider the real symmetric matrix Ω_0

$$\Omega_0 = \begin{pmatrix}
1 & 0.2 & 0.1 & 0.03 \\
0.2 & -0.3 & 0 & 0 \\
0.1 & 0 & -0.1 & 0 \\
0.03 & 0 & 0 & -0.5
\end{pmatrix}$$
(51)

which clearly has the special form given in equation (25). The G-eigenvalues of Ω_0 are obtained by solving the secular equation $\det(G\Omega_0 - \lambda \mathbb{1}_4) = 0$ and

given by $\lambda_0 = 0.921$, $\lambda_1 = 0.503$, $\lambda_2 = 0.366$, $\lambda_3 = 0.109$. It is found that the *G*-eigenvector $X_0 = (0.943, -0.303, -0.115, -0.067)$ belonging to the largest *G*-eigenvalue $\lambda_0 = 0.921$ is time-like (because its Minkowski norm is positive: $X_0^T G X_0 = 0.780$).

Minkowski norm is positive: $X_0^T G X_0 = 0.780$). A plot of $h(\lambda) = n_0 - \lambda - \sum_i \frac{n_i^2}{\lambda_i + \alpha_i}$ with $n_0 = 1$, $n_1 = 0.2$, $n_2 = 0.1$, $n_3 = 0.03$ and $\alpha_1 = -0.3$, $\alpha_2 = -0.1$, $\alpha_3 = -0.5$ associated with Ω_0 in (51) as a function of the continuous variable λ is given in Fig. 1. It is seen that $h(\lambda)$ is discontinuous at $\lambda = -\alpha_i$, i = 1, 2, 3 i.e., at 0.1, 0.3, and 0.5 on the λ -axis. It is seen that the G-eigenvalues of Ω_0 match exactly with the roots $\lambda_0 = 0.921, \lambda_1 = 0.503, \lambda_2 = 0.366, \lambda_3 = 0.109$ of $h(\lambda)$. Moreover the slope $h'(\lambda_0)$ is negative – implying that the associated G-eigenvector X_0 is time-like, in confirmation with the detailed analysis of subsection IIIB. Based on

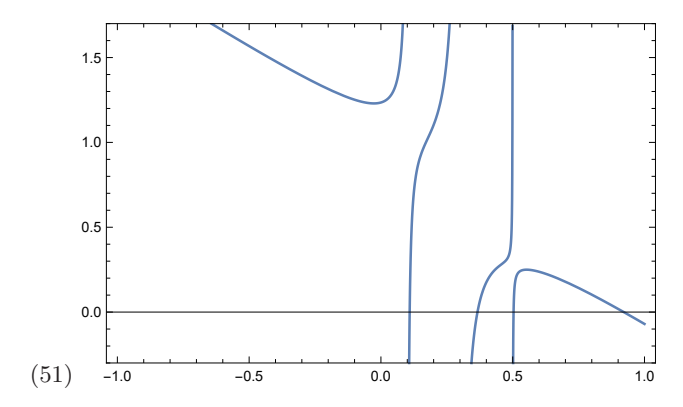


FIG. 1 (Colour online) Plot of $h(\lambda) = 1 - \lambda - \frac{0.04}{\lambda - 0.3} - \frac{0.01}{\lambda - 0.1} - \frac{0.009}{\lambda - 0.5}$, associated with the real symmetric matrix Ω_0 given by equation (51) as a function of λ . At $\lambda = 0.1$, 0.3, 0.5 the function $h(\lambda)$ exhibits singularities. Four zeros of the $h(\lambda)$ (which happen to be the *G*-eigenvalues Ω_0 given by equation (51)) occur at $\lambda_0 = 0.921, \lambda_1 = 0.503, \lambda_2 = 0.366, \lambda_3 = 0.109$. It is seen that the slope $h'(\lambda_0 = 0.921)$ is negative, confirming that the *G*-eigenvector belonging to the highest *G*-eigenvalue $\lambda_0 = 0.921$ is time-like.

this analysis it is seen that the real symmetric matrix Ω_0 of equation (51) gets transformed to its canonical form $\Omega_0^{Ic} = \text{diag}(0.921, 0.503, 0.366, 0.109)$. We thus obtain the Lorentz canonical form (see equation (41)) of the associated real matrix parametrization of the two-qubit density matrix:

$$\Lambda_{Ic} = \text{diag} (1, 0.739, 0.630, \pm 0.344).$$

The two-qubit density matrix ρ_{AB}^{Ic} (see equation (42)) is given by

$$\rho_{AB}^{Ic} = \frac{1}{4} (\sigma_0 \otimes \sigma_0 + 0.739 \,\sigma_1 \otimes \sigma_1$$

$$+0.630 \sigma_2 \otimes \sigma_2 \pm 0.344 \,\sigma_3 \otimes \sigma_3).$$
(52)

The canonical steering ellipsoid representing the set of all two-qubit states which are on the SL(2,C) orbit of ρ_{AB}^{Ic} of equation (52) is shown in Fig. 2.

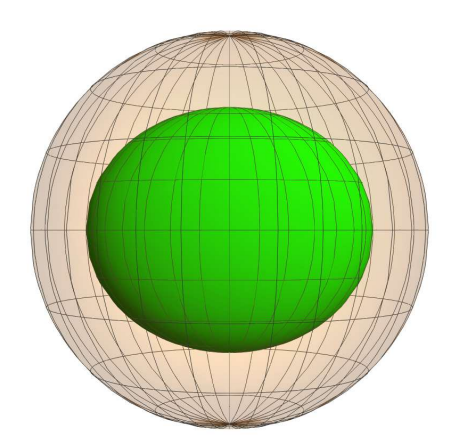


FIG. 2 (Colour online) Canonical steering ellipsoid representing the two-qubit states which are SL(2,C) equivalent to ρ_{AB}^{Ic} of equation (52). The ellipsoid is centered at the origin of the Bloch sphere with semi-axes $\sqrt{\frac{\lambda_1}{\lambda_0}}=0.739,\,\sqrt{\frac{\lambda_2}{\lambda_0}}=0.630$ and $\sqrt{\frac{\lambda_3}{\lambda_0}}=0.344$.

Example 2: Consider

$$\Omega_0 = \begin{pmatrix}
1 & 0.2 & 0.25 & 0 \\
0.2 & -0.3 & 0 & 0 \\
0.25 & 0 & -0.15 & 0 \\
0 & 0 & 0 & -0.04
\end{pmatrix}$$
(53)

which exhibits the form given by equation (25). We determine the G-eigenvalues of Ω_0 (see (53)) and obtain

$$\lambda_0 = 0.833, \ \lambda_1 = 0.414, \ \lambda_2 = 0.202, \ \lambda_3 = 0.04.$$
 (54)

The G-eigenvector

$$X_0 = (0.886, -0.332, -0.324, 0)$$

belonging to the largest G-eigenvalue $\lambda_0=0.833$ is found to be time-like i.e., it has positive Minkowski norm $X_0^T G X_0=0.569$.

A plot of the function

$$h(\lambda) = 0.2 - \lambda - \frac{0.04}{\lambda - 0.3} - \frac{0.0625}{\lambda - 0.15}$$
 (55)

associated with the matrix Ω_0 given by (53) as a function of λ is shown in Fig. 3. Note that $h(\lambda)$ has two discontinuities at 0.3 and 0.15. Three of the G-eigenvalues λ_0 , λ_1 , λ_2 of Ω_0 (see (54)) agree with the three zeros 0.202, 0.414, 0.833 of $h(\lambda)$. Moreover the slope h'(0.833) is negative – implying that the associated G-eigenvector X_0 is time-like. The remaining G-eigenvalue $\lambda_3 = 0.04$

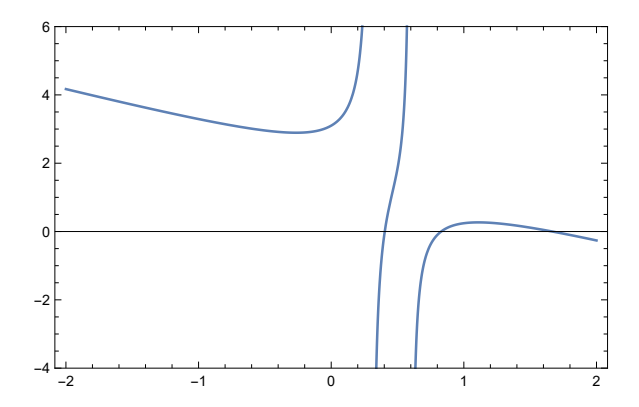


FIG. 3 (Colour online) Plot of $h(\lambda)$ given in equation (55) as a function of λ . It is seen that $h(\lambda)$ exhibits only two discontinuities at $\lambda=0.15,\,0.3$ and has three zeros at 0.202, 0.414, 0.833, which match identically with the G-eigenvalues of Ω_0 of Example 2 (see (53)). Root of the function $\phi_1(\lambda)=(\lambda-0.04)$ (see case (ii) of Table 1) determines the remaining G-eigenvalue is then determined by . It is also seen that the slope of h'(0.833) is negative, confirming that the G-eigenvector belonging to the largest G-eigenvalues $\lambda_0=0.833$ is time-like Minkowski four-vector.

is equal to the root of the polynomial $\phi_1(\lambda) = (\lambda - 0.04)$ (see case (ii) in Table 1).

The Lorentz canonical form of the real matrix parametrization of ρ_{AB} is given by

$$\Lambda_{Ic} = \text{diag} (1, 0.705, 0.492, \pm 0.219)$$
 (56)

and the density matrix corresponding to Ω_0 of (53) is given by (see equation (42))

$$\rho_{AB}^{Ic} = \frac{1}{4} (\sigma_0 \otimes \sigma_0 + 0.705 \,\sigma_1 \otimes \sigma_1 + 0.492\sigma_2 \otimes \sigma_2 \pm 0.219 \,\sigma_3 \otimes \sigma_3). \tag{57}$$

The canonical steering ellipsoid representing the set of all two-qubit states, which are on the SL(2,C) orbit of ρ_{AB}^{Ic} of equation (57) is displayed in Fig. 4.

Example 3: Let us consider

$$\Omega_0 = \begin{pmatrix}
0.596 & 0 & 0.148 & 0 \\
0 & -0.264 & 0 & 0 \\
0.148 & 0 & -0.183 & 0 \\
0 & 0 & 0 & -0.078
\end{pmatrix} (58)$$

for which we find the G-eigenvalues as

$$\lambda_0 = 0.533, \, \lambda_1 = 0.264, \, \lambda_2 = 0.246, \, \lambda_3 = 0.0786 \quad (60)$$

and the G-eigenvector belonging to the highest G-eigenvalue $\lambda_0 = 0.533$ is given by

$$X_0 = (0.920, 0, -0.391, 0).$$
 (61)

The Minkowski norm $X_0^T G X_0 = 0.694$ revealing that the G-eigenvector (given in equation (gev3)) associated

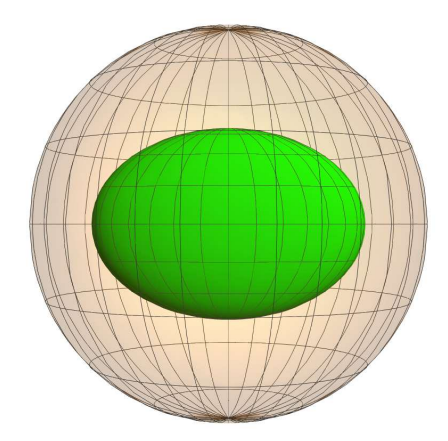


FIG. 4 (Colour online) Canonical steering ellipsoid representing the set of all two-qubit density matrices on the SL(2,C) orbit of ρ_{AB}^{Ic} of equation (57). The ellipsoid with semi-axes 0.705, 0.492, 0.219 is centered at the origin of Bloch sphere.

with the largest G-eigenvalue $\lambda_0 = 0.533$ of Ω_0 is time-like.

We have plotted the function $h(\lambda) = 0.596 - \lambda - \frac{0.148}{\lambda - 0.183}$ corresponding to Ω_0 of equation (63) in Fig. 5. It is seen that $h(\lambda)$ has one discontinuity at $\lambda = 0.183$ and two zeros at 0.246, 0.533, which match identically with the G-eigenvalues λ_1 , λ_0 given in equation (60). Remaining G-eigenvalues are found to be the roots of the polynomial $\phi_1(\lambda) = (\lambda - 0.264) (\lambda - 0.078)$ (see case (iii) of Table 1). The slope $h'(\lambda_0 = 0.533)$ of $h(\lambda)$ at its largest zero is negative and ascertains that the G-eigenvector belonging to the largest G-eigenvalue is time-like.

We obtain the Lorentz canonical form of the real parametrization Λ_{Ic} as

$$\Lambda_{Ic} = \text{diag} (1, 0.703, 0.679, \pm 0.384)$$
 (62)

and the corresponding $SL(2,\mathbb{C})$ canonical form of the twoqubit density matrix is given by

$$\rho_{AB}^{Ic} = \frac{1}{4} (\sigma_0 \otimes \sigma_0 + 0.704 \,\sigma_1 \otimes \sigma_1 + 0.679 \,\sigma_2 \otimes \sigma_2 \pm 0.384 \,\sigma_3 \otimes \sigma_3).$$
(63)

The canonical steering ellipsoid representing the set of all two-qubit states connected ρ_{AB}^{Ic} of equation (63) via $SL(2,\mathbb{C})$ transformations is displayed in Fig. 6.

Example 4: We present an example where the function $h(\lambda)$ has a single discontinuity and it leads to the SL(2,C) canonical form ρ_{AB}^{IIc} (see equation (44)) for the two-qubit density matrix. We consider the real symmetric matrix

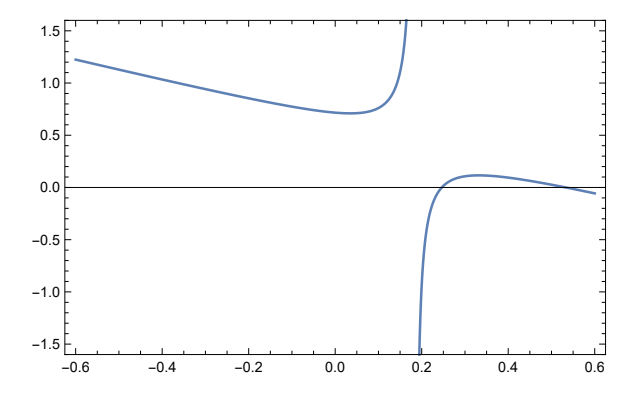


FIG. 5 (Colour online) Plot of $h(\lambda) = 0.596 - \lambda - \frac{0.148}{\lambda - 0.183}$ associated with Ω_0 given by equation (63). The function $h(\lambda)$ has a single discontinuity at $\lambda = 0.183$ and crosses the λ -axis twice. The roots of $h(\lambda)$ at 0.246 and 0.533 match with the G-eigenvalues λ_1 , λ_0 respectively (see equation (60)). Two more G-eigenvalues $\lambda_2 = 0.264$, $\lambda_3 = 0.264$ are the roots of the polynomical $\phi_1(\lambda) = (\lambda - 0.264) (\lambda - 0.078)$ (This corresponds to case (iii) of Table 1)). It is seen that h'(0.533) is negative, indicating the time-like nature of the the G-eigenvector X_0 corresponding to the largest G-eigenvalues $\lambda_0 = 0.533$

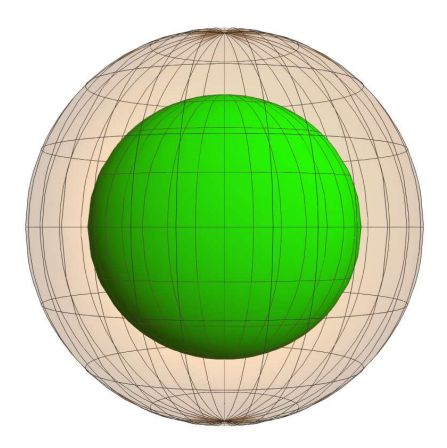


FIG. 6 (Colour online) Steering ellipsoid representing the set all two-qubit states having SL(2,C) equivalence with $\rho^{(3)}$. Semi-axes of the ellipsoid $a_1=0.7,\ a_2=0.68,\ a_3=0.38$.

given by

$$\Omega_0 = \frac{1}{36} \begin{pmatrix} 2 & 0 & 0 & 1\\ 0 & -1 & 0 & 0\\ 0 & 0 & -1 & 0\\ 1 & 0 & 0 & 0 \end{pmatrix}. \tag{64}$$

We find that the G-eigenvalues of Ω_0 are four fold degenerate with $\lambda_0 = \lambda_1 = \lambda_2 = \lambda_3 = 1/36$. Corresponding G-eigenvectors form a triad consisting of one null and

two space=like four-vectors:

$$X_0 = (1, 0, 0, -1), X_1 = (0, 1, 0, 0), X_2 = (0, 0, 1, 0).$$

We have plotted the associated function

$$h(\lambda) = \frac{1}{18} - \lambda - \frac{(1/36)^2}{\lambda}$$

in Fig. 7. It is evident that $h(\lambda)$ has one discontinuity at $\lambda = 0$; a single root at $\lambda = \frac{1}{36}$. The slope h'(1/36) is zero confirming that one of the G-eigenvectors is a null four-vector.

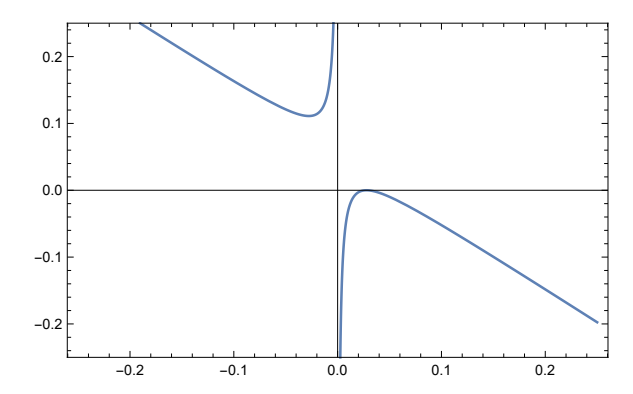


FIG. 7 (Colour online) Plot of $h(\lambda)$ associated with Ω_0 given by equation (wpi2). The function exhibits only one discontinuity at $\lambda=0$ and is zero at $\lambda=1/36$. The slope $h'(\lambda)$ at $\lambda=1/36$ is zero implying that one of the G-eigenvector must be a null four-vector.

The Lorentz canonical form of the real matrix Λ is given by

$$\Lambda_{IIc} = \begin{pmatrix}
1 & 0 & 0 & \frac{1}{2} \\
0 & \frac{1}{\sqrt{2}} & 0 & 0 \\
0 & 0 & -\frac{1}{\sqrt{2}} & 0 \\
0 & 0 & 0 & 0
\end{pmatrix}$$
(65)

and the associated $SL(2,\mathbb{C})$ canonical form of the twoqubit density matrix is given by

$$\rho_{AB}^{IIc} = \frac{1}{4} \left(\sigma_0 \otimes \sigma_0 + \frac{1}{\sqrt{2}} \sigma_1 \otimes \sigma_1 - \frac{1}{\sqrt{2}} \sigma_2 \otimes \sigma_2 \right) (66)$$

Geometrical representation of the set of all states which are SL(2,C) equivalent to the two-qubit density matrix given by equation (66) in terms of a shifted spheroid with semi-axes $\left(\frac{1}{\sqrt{2}}, \frac{1}{\sqrt{2}}, \frac{1}{2}\right)$ and center (0, 0, 1/2) is given in Fig. (8)).

VI. SUMMARY

We have investigated the two different types of Lorentz canonical forms for the 4×4 real-matrix parametrization Λ of a two-qubit density matrix $\rho_{AB}=\frac{1}{4}\sum_{\mu=0}^4\Lambda_{\mu\nu}\,\sigma_{\mu}\otimes$

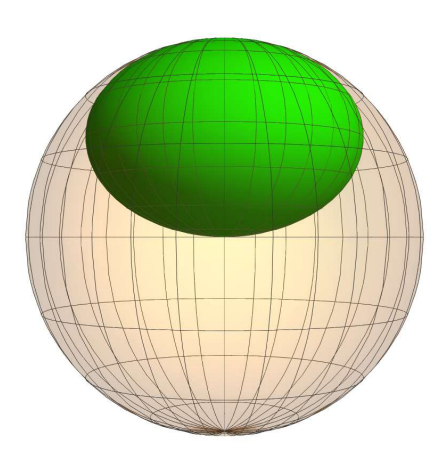


FIG. 8 (Colour online) Canonical steering ellipsoid representing the set of all SL(2,C) equivalent two-qubit states ρ_{AB}^{IIc} of equation (66) is a spheroid centered at (0, 0, 1/2) with its semi-axes $\left(\frac{1}{\sqrt{2}}, \frac{1}{\sqrt{2}}, \frac{1}{2}\right)$

 σ_{ν} . Transormation of two-qubit density matrix under local SL(2,C) operations results in Lorentz transformation on the real matrix parametrization Λ . Based on the observation that Λ transforms the set of four-vectors

REFERENCES

Avron, J. E. G. Bisker and O. Kenneth, (2007), "Visualizing Two Qubits," J. Math. Phys. 48, 102107

Bengtsson, I., and K. Życzkowski (2006), Geometry of Quantum States: An Introduction to Quantum Entanglement (Cambridge University Press, Cambridge)

Bloch, F. (1946), "Nuclear induction," Phys. Rev. ${\bf 70},~460-474$

Gamel, O., (2016), "Entangled Bloch spheres: Bloch matrix and two-qubit state space," Phys. Rev. A 93, 062320

Gopala Rao, A. V., K. S. Mallesh and Sudha, (1998a), "On the algebraic characterization of a Mueller matrix in polarization optics: I. Identifying a Mueller matrix from its N matrix," J. Mod. Opt. **45**, 955-987

Gopala Rao, A. V., K. S. Mallesh and Sudha, (1998b), "On the algebraic characterization of a Mueller matrix in polarization optics: II. Necessary and sufficient conditions for Jones-derived Mueller matrices," J. Mod. Opt. 45, 989-999 with non-negative Minkowski norm into itself, it is shown that the spectral properties of the symmetric matrix $\Omega = \Lambda^T G \Lambda$, where G = diag(1, -1, -1, -1) denotes the Minkowski metric, determines the Lorentz canonical forms of Λ . This leads us to a detailed mathematical analysis, based on Lagrange multiplier approach, to discern the zeros and discontinuities of a function $h(\lambda)$ constructed with the elements of the matrix Ω . It is shown that the zeros and discontinuities of the function $h(\lambda)$ discern the nature of eigenvalues and eigenvectors of the matrix $G\Omega$. This detailed exploration leads to two different types of Lorentz canoncial forms Λ_{Ic} , Λ_{IIc} for the real matrix parametrization corresponding to the respective SL(2,C) canonical forms ρ_{AB}^{Ic} , ρ_{AB}^{IIc} of the two-qubit density matrices. The Lorentz canonical forms Λ_{Ic} , Λ_{IIc} enable geometric picturization of the set of all SL(2,C) equivalent density matrices $\rho_{AB}^{Ic},\,\rho_{AB}^{IIc}$ in terms of canonical steering ellipsoids inscribed inside the Bloch sphere.

VII. ACKNOWLEDGMENTS

Sudha, BNK and ARU are supported by Department of Science and Technology (DST), India, No. DST/ICPS/QUST/ 2018/107; HSK is funded by NCN Poland, ChistEra-2023/05/Y/ST2/00005 under the project Modern Device Independent Cryptography (MoDIC); ASH acknowledges funding from Foundation for Polish Science (IRAP Project, ICTQT, contract no. MAB/2018/5, cofinanced by EU within Smart Growth Operational Programme).

Goyal, S. K., B. N. Simon, R. Singh and S. Simon (2016), "Geometry of the generalized Bloch sphere for qutrits," J. Phys. A: Math. Theor. **49**, 165203

Horodecki, R., and M. Horodecki (1996), "Information-theoretic aspects of inseparability of mixed states," Phys. Rev. A 54, 1838

Jevtic, S., M. F. Pusey, D. Jennings and T. Rudolph, (2014), "Quantum steering ellipsoids," Phys. Rev. Lett. 113, 020402

Kimura, G and A. Kossakowski (2003a), "The Bloch-vector space for *n*-level systems: the Spherical-Coordinate Point of View," Open Syst. Inf. Dyn. **12**, 207

Milne, A., D. Jennings, H. Wiseman and T. Rudolph (2014), "Quantum steering ellipsoids, extremal physical states and monogamy," New J. Phys. 16, 083017

Rau, A. R. P (2021), "Symmetries and geometries of qubits, and their uses," Symmetry 13, 1732

Srnivasa Rao, K. N. (1988), The Rotation and Lorentz Groups

TABLE I The polynomial functions $\phi_1(\lambda)$, $g(\lambda)$ and $h(\lambda)$ in 20 different physical cases

and Their Representations for Physicists, (Wiley Eastern, New Delhi)

 $n_0 - \lambda$

 $n_0 - \lambda$

Sudha, H. S. Karthik, R. Pal, K. S. Akhilesh, S. Ghosh, $g(\lambda)$ S. Mallesh and A. R_h Usha Devi, (2020), "Canonical Sl. No. Case $\phi_1(\lambda)$ perations," Phys. $n_1, n_2, n_3 \neq 0$ (i) Rev. A 102, 052419 $\begin{array}{c} n_0 - \lambda - \sum_i \frac{n_i}{(\alpha_i + \lambda)} \\ 2), \quad Relativity - \frac{1}{(\alpha_2 + \lambda)} \\ - \frac{1}{(\alpha_2 + \lambda)} \end{array} ial \quad Theory, \quad (Ams-$ (A) $\alpha_1 \neq \alpha_2 \neq \alpha_3$ 1 $(\alpha_1 + \lambda)(\alpha_2 + \lambda)(\alpha_3 + \lambda)$ (1972), Relativity; n_0 $(\alpha + \lambda)$ $(\alpha + \lambda)(\alpha_3 + \lambda)_{N_c}$ (B1) $(\alpha + \lambda)$ $\alpha_1 = \alpha_2 = \alpha \neq \alpha_3$ $n_0 - \lambda - \frac{n_1^2}{(\alpha_1 + \lambda)} - \frac{n_2^2 + n_3^2}{(\alpha + \lambda)}$, Dehaene and Q. Kenneth (B2) $\alpha_1 \neq \alpha_2 = \alpha_3 = \alpha$ $(\alpha + \lambda)$ $(\alpha + \lambda)(\alpha_1 + \lambda)$ $(\alpha + \lambda)(\alpha_2 + \lambda)$ F., J (2001), "Local fil-(B3) $\alpha_1 = \alpha_3 = \alpha \neq \alpha_2$ $(\alpha + \lambda)$ on two (qub) ts," (Phys) Rev. A **64**, 064104 $n_0 - \lambda - \frac{n_1^2 + n_2^2 + n_3^2}{n_1^2 + n_3^2}$ $(\alpha + \lambda)^2$ (C) $\alpha_1 = \alpha_2 = \alpha_3 = \alpha$ $(\alpha + \lambda)$ $(\alpha + \lambda)$ Verstraete, F., 2002), Ph.D thesis., (Katholieke Universiteit Leuven) (ii) $n_1, n_2 \neq 0, n_3 = 0$ $(\alpha_1 + \lambda)(\alpha_2 + \lambda)$ (A) $\alpha_1 \neq \alpha_2 \neq \alpha_3$ $(\alpha_3 + \lambda)$ (B1) $\alpha_1 = \alpha_2 = \alpha \neq \alpha_3$ $(\alpha_3 + \lambda)(\alpha + \lambda)$ $(\alpha + \lambda)$ $(\alpha + \lambda)$ (B2) $\alpha_1 \neq \alpha_2 = \alpha_3 = \alpha$ $(\alpha_1 + \lambda)(\alpha + \lambda)$ $(\alpha + \lambda)$ $(\alpha + \lambda)(\alpha_2 + \lambda)$ (B3) $\alpha_1 = \alpha_3 = \alpha \neq \alpha_2$ $(\alpha + \lambda)^2$ (C) $\alpha_1 = \alpha_2 = \alpha_3 = \alpha$ $(\alpha + \lambda)$ $n_0 - \lambda$ – (iii) $n_1 = n_3 = 0, n_2 \neq 0$ (A) $\alpha_1 \neq \alpha_2 \neq \alpha_3$ $(\alpha_1 + \lambda)(\alpha_3 + \lambda)$ $(\alpha_2 + \lambda)$ $\alpha_1 = \alpha_2 = \alpha \neq \alpha_3$ $(\alpha + \lambda)(\alpha_3 + \lambda)$ (B1) $(\alpha + \lambda)$ $n_0 - \lambda$ $(\alpha_1 + \lambda)(\alpha + \lambda)$ (B2) $\alpha_1 \neq \alpha_2 = \alpha_3 = \alpha$ $(\alpha + \lambda)$ n_0 $(\alpha + \lambda)^2$ (B3) $\alpha_1 = \alpha_3 = \alpha \neq \alpha_2$ $(\alpha_2 + \lambda)$ $n_0 - \lambda$ $(\alpha + \lambda)^2$ (C) $\alpha_1 = \alpha_2 = \alpha_3 = \alpha$ $(\alpha + \lambda)$ $n_0 - \lambda$ (iv) $n_1 = n_2 = n_3 = 0$ (A) $\alpha_1 \neq \alpha_2 \neq \alpha_3$ $(\alpha_1 + \lambda)(\alpha_2 + \lambda)(\alpha_3 + \lambda)$ $n_0 - \lambda$ 1 (B1) $\alpha_1 = \alpha_2 = \alpha \neq \alpha_3$ $(\alpha + \lambda)^2(\alpha_3 + \lambda)$ 1 $n_0 - \lambda$ $(\alpha + \lambda)^2(\alpha_1 + \lambda)$ (B2) $\alpha_1 \neq \alpha_2 = \alpha_3 = \alpha$ 1 $n_0 - \lambda$

1

1

 $(\alpha + \lambda)^2(\alpha_2 + \lambda)$

 $(\alpha + \lambda)^3$

(B3)

(C)

 $\alpha_1 = \alpha_3 = \alpha \neq \alpha_2$

 $\alpha_1 = \alpha_2 = \alpha_3 = \alpha$